Using composite phenotypes to reveal hidden physiological heterogeneity and model oxygen saturation variation of high altitude acclimatization in a Chinese Han longitudinal cohort

Yi Li[1], Yi Wang[1], Menghan Zhang[1], Yanyun Ma[1], Kun Wang[1], Xiaoyu Liu[1], Meng Hao[1], Chang Sun[1], Xiaofeng Wang[1,2], Xingdong Chen[1,2], Yao Zhang[3], Wenyuan Duan[4], Longli Kang[3], Bin Qiao[4], Jiucun Wang[1,2], Li Jin[1,2*]

[1] Ministry of Education Key Laboratory of Contemporary Anthropology, Collaborative Innovation Center for Genetics and Development, School of Life Sciences and Human Phenome Institute, Fudan University, Shanghai, China

[2] Fudan-Taizhou Institute of Health Sciences, Taizhou, China

[3] Key Laboratory of High Altitude Environment and Genes Related to Diseases of Tibet Autonomous Region, School of Medicine, Xizang Minzu University, Xianyang, China.

[4] Institute of Cardiovascular Disease, General Hospital of Jinan Military Region, Jinan, Shandong, China.

*Corresponding authors:

Dr. Li Jin, School of Life Sciences, Fudan University, 2005 Songhu Road, Shanghai 200438, China.

Tel: 8602151630607. Fax: 8602151630607. Email: lijin@fudan.edu.cn

ABSTRACT

Altitude acclimatization is the physiological process of the human body adjusting to the decreased availability of oxygen. Since several physiological processes are involved and the relation among them is complicated, analyses of single-traits is insufficient in revealing the complex mechanism of high altitude acclimatization. In this study, we examined whether these physiological responses could be studied as composite phenotypes which are represented by a linear combination of physiological traits. We developed a strategy which combines both spectral clustering and Partial Least Squares Path Modeling (PLSPM) to define composite phenotypes based on a cohort study of 883 Chinese Han males. And we captured 14 composite phenotypes from 28 physiological traits of high altitude acclimatization. Using these composite phenotypes, we applied k-means clustering to reveal hidden population physiological heterogeneity in high altitude acclimatization. Furthermore, we employed multivariate linear regression to systematically model (Model 1 and Model 2) oxygen saturation (SpO_2) changes in high altitude acclimatization and evaluated the model fitness performance. And composite phenotypes based Model 2 has better fitness than single-traits based Model 1 in all measurement indices. Therefore, this new strategy of defining and applying composite phenotypes can be considered as a general strategy of complex traits research, which may also shed light on genetic loci discovery and phenome analyses.

INTRODUCTION

Altitude acclimatization is the physiological process of the human body adjusting to the decreased availability of oxygen[1]. It comprises of several physiological responses in the body, including ventilation function, cardiac function, oxygen delivery function, hematology, muscle structure and metabolism, oxygen consumption and so on[2,3]. The most important physiological responses are in the cardiorespiratory and the hematology system[2]. Oxygen saturation (SpO_2) reflect the most straightforward physiological changes [2,4-7]. The SpO_2 quickly decreased in three days in lowlanders ascending directly to 4,300 m, followed by a rise over weeks at altitude[1,2,8,9]. Another well-known physiological change is the hemoglobin concentration in the blood [1,8-10]. It is also known that individuals vary in both the speed and extent to altitude acclimatization[1,11,12]. The variations of responses across individuals provide an opportunity to explore the mechanism of altitude acclimatization[1,9,11].

Since several physiological processes are involved and the relation among them is complicated, analyses of single-traits are insufficient to capture the complex mechanism of high altitude acclimatization[1,4,9]. Therefore, analysis of composite phenotypes, i.e. combinations of physiological phenotypes could become a promising alternative[13-15]. There are several methods to extract composite phenotypes from multiple traits, such as Principal Component Analysis (PCA)-based methods[14,16,17] and Partial Least Squares (PLS)-based methods[9,18,19]. PLS-based methods have better performance than PCA-based methods[18,19]. Partial Least Squares Path Modeling (PLSPM) is the PLS-based approach to Structural Equation Modeling[20-22], which can also be viewed as a method for analyzing multiple relationships between groups of variables. In the PLSPM framework, there are generally two ways to define composite

phenotypes, i.e., latent variables[9,19-22]: one is using the prior knowledge and the other is using data-driven methods such as spectral clustering[23,24].

Here, we conducted a two-phase longitudinal study of high altitude acclimatization (baseline and chronic phase) in a large sample of 883 Chinese Han young males. Overall 28 physiological phenotypes were collected from these individuals at each phase. First, we extracted composite phenotypes from physiological phenotypes in high altitude acclimatization by introducing a data-driven strategy constituting spectral clustering[23,24] and PLSPM[20,21] algorithm. Second, using these composite phenotypes, we revealed hidden population physiological heterogeneity in high altitude acclimatization using k-means clustering[25]. Third, we modeled the changes of SpO_2 during high altitude acclimatization using multivariate linear regression[26], and further evaluated the advantages of composite phenotypes over single phenotypes. The workflow was summarized in **Fig. 1**, which is also the design of this study. The term phenotype used in this manuscript are referred to as "The Extended Phenotype[27]".

METHOD

Study overview

To explore the physiological changes at two phases (baseline and chronic, **Table 1**) of high altitude acclimatization, the longitudinal data were transformed into change data[28]. To extract composite phenotypes from the 28 physiological traits, spectral clustering[23,24,29] was applied firstly (**Fig. 1**). Based on the spectral clustering results (composite phenotype structure, **Fig. 2**), PLSPM[20] was applied to construct and estimate the 14 composite phenotypes (**Table2, Fig. 3**). Using the 14 composite phenotypes, we applied k-means clustering algorithm[23,25] to explore physiological

heterogeneity in high altitude acclimatization (**Fig. 4**). To further investigate the physiological patterns of the two groups, pairwise Pearson correlation heatmap was shown (**Fig. 5**). To model how physiological traits systematically relate to SpO_2 changes in high altitude acclimatization process, two multivariate linear regression models [26] were constructed. Finally, to evaluate the fitness of two models, AIC[30,31], BIC[31,32], 10-fold CV[33] RMSE[34] and leave-one-out RMSE were measured (**Table 3**). In summary, firstly we have a problem in biology and then we tried to solve it using several effective statistical methods.

All the computation process of this study were realized in R (v3.3.1)[35] and the related figures were generated by Matlab (R2015b)[36], 'ggplot2'[37], 'igraph'[38] R packages. The computation process of composite phenotype scores was completed by 'plspm'[20] R package. The k-means clustering was completed by 'factoextra'[39] and 'NbClust'[40] R package. The multivariate linear regression models were calculated by 'stats' R package.

Exploring relationship of phenotypes by spectral clustering

The longitudinal data of high altitude acclimatization were firstly transformed into change data[28]. All the 28 physiological traits have significant (under Bonferroni correction[41]) changes from baseline to chronic phase at 4,300m highland. And the p values were calculated by Wilcoxon Rank-Sum Test[42] (**Table 1)**. Based on the change data of high altitude acclimatization, spectral clustering[23,24] was applied. The similarity matrixs in this study were the absolute values of spearman correlation coefficient [43] matrixs of 28 physiological changes from baseline to chronic phase for high altitude acclimatization. The affinity matrixs were computed by applying a k-nearest neighbor filter [44] to build a representation of a graph connecting just the closest dataset points.

To compute the graph Laplacian matrix, there is also a need to get the degree matrix where each diagonal value is the degree of the respective vertex and all other positions are zero[24]. To choose the best number of spectral clustering, the eigenvalue gap (difference between consecutive eigenvalues of Laplacian matrix, **Supplementary Fig. 1**) was maximized[29]. And the spectral clustering results were the composite phenotype structure (**Fig.1** and **Fig. 2**).

Defining composite phenotypes by PLSPM

Based on the composite phenotype structure, PLSPM [20,21] was further applied to construct composite phenotypes. And the latent variable scores[20,22] were calculated to estimate these composite phenotypes. As the 28 physiological traits were clustered as 14 groups, there were also 14 composite phenotypes (LV1, LV2… LV13, LV14) accordingly. PLSPM is claimed to explain at best the residual variance of the latent variables and potentially also of the manifest variables in any regression run in the model without strong assumptions [22]. To check the PLSPM blocks' unidimensionality, the Cronbach's alpha, Dillon-Goldstein's rho and the first eigenvalue of the indicators' correlation matrix were calculated [20,22]. Each composite phenotype captures a specific aspect of high altitude acclimatization (**Table 2**, **Fig. 3** and **Supplementary Fig. 2**).

Revealing physiological heterogeneity by k-means

Based on the 14 composite phenotypes, k-means clustering was applied to explore physiological heterogeneity in high altitude acclimatization (**Fig. 4**). The optimal number of clusters is 2 (**Supplementary Fig. 3**) following the majority rule of 26 indices[40]. The silhouette plot (**Supplementary Fig. 4**) for k-means clustering also showed that observations are well clustered [45]. Thus the 883 Chinese Han young males were clustered into two groups (group1 with 508 individuals and group2 with 375

individuals, **Fig. 4**) based on the 14 composite phenotypes of high altitude acclimatization. To further investigate the physiological patterns of the two groups, pairwise Pearson correlation [46] heatmap was shown (**Fig. 5**).

Modeling oxygen saturation variation by multivariate linear regression

To model how physiological traits systematically relate to SpO_2 changes in high altitude acclimatization process, two multivariate linear regression models [26] were constructed. Model 1 is constructed by original 28 physiological traits changes from baseline to chronic phase at 4300m highland and SpO_2 is the dependent variable (Y). Model 2 is constructed by 13 composite phenotypes (excluding LV13, i.e., SpO_2) of high altitude acclimatization, and SpO_2 is still the dependent variable (Y). To evaluate the fitness of two models, AIC [30,31], BIC[31,32], 10-fold CV[33] RMSE[34] and leave-one-out RMSE were measured (**Table 3**). We also employed Wilcoxon Rank-Sum Test [42] to compare the 10-fold CV MSE and leave-one-out MSE of two models (Model 1 and Model 2).

Participants

We conducted a longitudinal cohort measurement design to investigate the responses of 28 physiological traits during high altitude acclimatization. The studied subjects were first assembled at a location with an altitude of 50 m (in China) for 10–14 days, and then they arrived at highland of above 4,300 m (in China) by train. The study is comprised of two phases: baseline phase (before going to highland) and chronic phase (living at highland for about 1 month). A structured questionnaire and physiological examination for the subjects were carried out at two phases of high altitude acclimatization respectively. The subjects with cancer, diabetes and coronary heart disease were not included in this study. Overall 883 healthy Chinese Han young

males aged from 17 to 36 years old were recruited. The research was approved by the Human Ethics Committee of Fudan University and written informed consent was obtained from each participant and their guardians over 18 years old.

Physiological measurements

All the subjects (883 samples, 28 traits) were measured by physicians in General Hospital of Jinan Military Region, who were previously trained to administer a questionnaire and a physical examination. The systolic blood pressures (SBP) and diastolic blood pressures (DBP) were calculated by mean of twice measurement of a standardized mercury sphygmomanometer. Maximal vital capacity (FVC) were measured by SPIDA5. Heart rate (HR) was measured by mean of twice radial pulse, SPO_2 was measured by Nellcor NPB-40. The body temperature (Temperature) was measured by thermometer. The blood specimens were drawn after overnight fasting for complete blood count measurement by three classification haemacytometer analyzer (Model CA-800; CIS, Japan). The blood routine indices include red blood cell count (RBC, $\times 10^{12}$/L), hemoglobin (HGB, g/L), hematocrit (HCT, %), mean corpuscular volume (MCV, fL), mean corpuscular hemoglobin (MCH, pg), mean corpuscular hemoglobin concentration (MCHC, g/L), white blood cell counts (WBC, $\times 10^{9}$/L), lymphocyte percentage (LYM%), absolute lymphocyte count (LYM#, $\times 10^{9}$/L), blood platelet (PLT, $\times 10^{9}$/L), mean platelet volume (MPV, fL), plateletcrit (PCT, fL), platelet distribution width (PDW, fL). The blood biochemical indices were measured by the automatic biochemical analyzer (Model 7060; Hitachi Ltd., Japan), including glutamate pyruvate transaminase (ALT, U/L), glutamic oxalacetic transaminase (AST, U/L), total bilirubin (TBIL, umol/L), direct bilirubin (DBIL, umol/L), blood urea nitrogen (BUN, mmol/L) and creatinine (CREA, umol/L). AST/ALT ratio and indirect bilirubin (IBIL,

umol/L) were calculated indices. The Lake Louise score (LLS) system scores[47] were also collected in two phases. The LLS questionnaire consists of five items: headache, dizziness, gastrointestinal symptoms, fatigue/weakness and difficulty sleeping. Each item was rated on a four-point scale (0= not at all, 1=mild, 2=moderate and 3=severe). Single item scores are added up and the maximal score is 15.

RESULTS

Exploring relationship of phenotypes in high altitude acclimatization

In this study, we collected the 28 physiological traits from 883 Chinese Han young males at baseline (before going to highland) and chronic (living at highland for about 1 month) phases of high altitude acclimatization (**Table 1**). The studied subjects were first assembled at a location with an altitude of 50 m (in China) for 10–14 days, and then they arrived at highland of above 4,300 m (in China) by train. The subjects with cancer, diabetes and coronary heart disease were not included in this study. Overall 883 healthy Chinese Han young males aged from 17 to 36 years old were recruited. All the 28 physiological traits show significant (Bonferroni correction) changes from baseline to chronic phase at 4,300m highland. These results indicate that a series of physiological phenotypes are involved in high altitude acclimatization process[1,2,9]. Since we are mainly concerned on the changes of these phenotypes, the longitudinal data were transformed into change data[28] using $\text{Measure}_{\text{chronic-baseline}} = \text{Measure}_{\text{chronic}} - \text{Measure}_{\text{baseline}}$. These data were used in subsequent analyses.

By analyzing the correlation between pairwise phenotypes, we found the phenotypes are structured **(Fig. 2)**. For example, RBC, HGB and HCT have strong correlation with each other; and RBC almost has no correlation with LLS and SPO_2.

To further explore the relationship of phenotypes, spectral clustering algorithm[23,24] was applied to group these 28 physiological phenotypes. To determine the number of clusters, the one with maximum eigenvalue gap (**Supplementary Fig. 1**) was chosen[29]. The correlation heatmap (**Fig. 2**) showed the spectral clustering results of 28 physiological phenotypes, and they were clustered into 14 groups (i.e. composite phenotype structure, **Fig. 2**).

Defining composite phenotypes of high altitude acclimatization

Based on the revealed aforementioned structure, PLSPM[20-22] was applied to extract composite phenotypes of high altitude acclimatization. Overall 14 composite phenotypes were extracted as the latent variables[20] (LV1, LV2… LV13, LV14). Each composite phenotype is a linear combination of their manifest variables [21], and captures a specific aspect of high altitude acclimatization (**Fig. 3, Table 2** and **Supplementary Fig. 2**). The LV5 explained the variance of RBC, HCT and HGB, which mainly reflect the number of red cells (Dillon-Goldstein's rho = 0.93, **Table 2 and Fig. 3**). The Dillon-Goldstein's rho focuses on the variance of the sum of variables in the block of latent variable[20,22]. The LV6 explained the variance of MCH, MCHC, MPV and MCV, which reflect the hemoglobin concentration. As the changes of MCH and MCHC were negatively related to MPV and MCV, we changed both MCH and MCHC signs to keep loadings positive[20]. The LV12 is equivalent to single-phenotype LLS and the LV13 represents single-phenotype SPO_2.

Revealing physiological heterogeneity in high altitude acclimatization

To explore physiological heterogeneity in high altitude acclimatization, we applied k-means clustering algorithm[23,25] on individuals using the 14 composite phenotypes. Thus the 883 individuals could be clustered into two groups (group 1 with 508

individuals and group 2 with 375 individuals, **Fig. 4**, **Supplementary Fig. 4** and **Supplementary Fig. 5**) based on the 14 composite phenotypes of high altitude acclimatization. The separation of two groups of the individuals are mainly contributed by hemoglobin concentration (LV6, Wilcox Rank Sum test's pvalue = 3.36×10^{-90}), number of red cells (LV5) and number of platelets (LV7) (**Supplementary Table 1** and **Supplementary Fig. 5**). The results demonstrate physiological heterogeneity in high altitude acclimatization among these sampled individuals, especially in the phenotypes related with oxygen carrying capacity[1,48,49] including hemoglobin concentration, number of red cells, platelet counts and so on. The increases in red cell number and hemoglobin concentration improve the oxygen carrying capacity of the blood to compensate for the reduction in oxygen saturation[1,50,51].

To further characterize the relationship of the 14 composite phenotypes in each group, we calculated the pairwise Pearson correlation[46] (**Fig. 5)**. For instance, there is significant correlation (Pearson's r = 0.12, pvalue = 0.006, **Supplementary Table 2**) between LV6 and LV13 in group 1, but no correlation between them in group 2 (Pearson's r = -0.03, pvalue = 0.51, **Supplementary Table 3**). To compare the difference of these two Pearson correlation coefficient, fisher's z transformation[52-55] were applied (pvalue=0.02, **Supplementary Table 4)**. There is negative correlation (Pearson's r = -0.2) between LV5 and LV7 in group 1, while in contrast, we observed positive correlation (Pearson's r = 0.17, fisher's z transformation pvalue =5.58×10^{-8}) between them in group 2. Thus we can compare the correlation networks of multiple physiological traits intuitively and focus on composite phenotypes not their manifest variables.

Modeling oxygen saturation variation of high altitude acclimatization

Oxygen saturation (SpO_2) reflect the most straightforward physiological change of high altitude acclimatization[2,4,5,7]. To model how other physiological traits systematically relate to SpO_2 changes in high altitude acclimatization process, we constructed two multivariate linear regression models. Model 1 is constructed by original 28 physiological traits changes from baseline to chronic phase at 4,300m highland and SpO_2 is the dependent variable (Y). To compare with this model, Model 2 is constructed by 13 composite phenotypes (excluding LV13, i.e., SpO_2) of high altitude acclimatization.

To evaluate the goodness of fit of two models, the Akaike information criterion (AIC)[30,31], Bayesian information criterion (BIC)[31,32], 10-fold cross validation (CV)[33] root-mean-square error (RMSE)[34] and leave-one-out RMSE were measured (**Table 3**). Model 2 has better fitness than Model 1 in all measurement indices (**Table 3**), suggesting that the composite phenotypes is better performed in capturing variation of high altitude acclimation. From the multivariate regression result of Model 2, we also found that LV12 (LLS) is the most significant ($\beta = -0.29$, $\text{pvalue} = 0.04$, **Supplementary Table 5**) trait that influence SpO_2. SpO_2 has been well studied as predictors/indicators of AMS or LLS[1,2,4,10,56-59]. And those individuals who successfully maintain their oxygen saturation at rest, most likely do not develop AMS[2,4,57].

DISCUSSION

In this study, we developed a data-driven strategy (**Fig. 1**) to extract composite phenotypes from multiple physiological phenotypes of high altitude acclimatization in a large-scale Chinese Han longitudinal cohort. We first explore the relationship of phenotypes of high-altitude acclimatization. And then we extracted 14 composite phenotypes from 28 physiological traits changes of high-altitude acclimatization. This

strategy could be applied to other complex traits, for example, immune diseases, cardio metabolic traits or other complex diseases.

Altitude acclimatization comprises a number of physiological responses to mitigate the effects of hypoxia[1,7]. There are many methods to analyze longitudinal data, such as linear mixed models[60] and data transformation[28]. Since we are mainly concerned on the changes of these phenotypes, transforming the longitudinal data into change data is also a promising alternative[2,9,28,61]. Thus the transformed data was used in this study.

Since individual single-traits are insufficient to reflect the complex mechanism of high altitude acclimatization[1,4,9], analysis of composite phenotypes could become a promising alternative[13-15]. Among several methods, PLS-based composite phenotypes have relatively interpretable biological meanings[9]. In particular, PLSPM can also be viewed as a method for analyzing multiple relationships between blocks of variables[20].

Generally, there are two ways to define composite phenotypes in PLSPM framework[9,22]: one is using the prior specific domain knowledge and the other is using some data-driven methods like clustering. In our study, we employed the generalized standard spectral clustering[23,24] to find the composite phenotype structure (**Fig. 2**) for high-altitude acclimatization.

This study included 28 physiological phenotypes which covered respiratory function, cardiac function, oxygen delivery function, hematology, oxygen saturation, kidney function, liver function, LLS and so on. However, there are still traits not involved in this study, such as muscle metabolism, oxygen consumption, electrocardiogram, electroencephalogram, organism metabolism and so on. And the data of this study was collected at two time points of high altitude acclimatization, which may be incomplete. The subjects in this study are all young males, the

physiological responses of females may be quite different. More importantly, other factors such as genetic variations, should be studied to further understand potential physiological mechanism of high altitude acclimatization[4,7].

In summary, we have developed a strategy constituting both spectral clustering and PLSPM to define composite phenotypes. And we effectively used this strategy to capture 14 composite phenotypes from 28 physiological phenotypes of high altitude acclimatization. The 14 composite phenotypes have clear meaning in physiology and explain most of variance in statistics. Based on these composite phenotypes, we first observed physiological heterogeneity among individuals in high altitude acclimatization. In addition, we compared the performance of composite phenotypes and regular phenotypes in predicting SpO_2 changes. Both analyses showed that the composite phenotypes is better performed in capturing variation of high altitude acclimation. To conclude, this new strategy of defining and applying composite phenotypes can be considered as a general strategy of complex traits research[62], especially in phenome analyses[63,64].

ACKNOWLEDGEMENTS

This research was supported by National Science Foundation of China (31330038, 31521003, 31460286), Ministry of Science and Technology (2015FY1117000), Science and Technology Committee of Shanghai Municipality (16JC1400500), Shanghai Municipal Science and Technology Major Project (2017SHZDZX01) and the 111 Project (B13016). The computations involved in this study were supported by the Fudan University High-End Computing Center.

CONTRIBUTIONS

YL and LJ conceived the idea and contributed to writing of the paper. YL, YW, MHZ and LJ contributed the theoretical analysis. YL, YYM, KW, YZ, LLK, XDC, WYD, BQ, JCW and LJ contributed the data collection and data cleaning. YL, YW, MHZ, YYM, KW, XYL, WLP, CS, JCW and LJ contributed to scientific discussion and manuscript writing. YL and LJ contributed to final revision of the paper.

COMPETING INTERESTS: The authors declare no competing financial interests.

FUNDING: This research was supported by National Science Foundation of China (31330038, 31521003, 31460286), Ministry of Science and Technology (2015FY1117000), Science and Technology Committee of Shanghai Municipality (16JC1400500), Shanghai Municipal Science and Technology Major Project (2017SHZDZX01) and the 111 Project (B13016).

REFERENCE

1 West, J. B., Schoene, R. B., Luks, A. M. & Milledge, J. S. *High altitude medicine and physiology 5E*. (CRC Press, 2012).

2 Muza, S. R., Beidleman, B. A. & Fulco, C. S. Altitude preexposure recommendations for inducing acclimatization. *High Alt Med Biol* **11**, 87-92, doi:10.1089/ham.2010.1006 (2010).

3 Martin, D. S., Levett, D. Z., Grocott, M. P. & Montgomery, H. E. Variation in human performance in the hypoxic mountain environment. *Exp Physiol* **95**, 463-470, doi:10.1113/expphysiol.2009.047589 (2010).

4 West, J. B., American College of, P. & American Physiological, S. The physiologic basis of high-altitude diseases. *Ann Intern Med* **141**, 789-800 (2004).

5 Martin, D. S. *et al.* Systemic oxygen extraction during exercise at high altitude. *Br J Anaesth* **114**, 677-682, doi:10.1093/bja/aeu404 (2015).

6 Peacock, A. J. & Jones, P. L. Gas exchange at extreme altitude: results from the British 40th Anniversary Everest Expedition. *European Respiratory Journal* **10**, 1439-1444, doi:10.1183/09031936.97.10071439 (1997).

7 West, J. B. Physiological Effects of Chronic Hypoxia. *N Engl J Med* **376**, 1965-1971, doi:10.1056/NEJMra1612008 (2017).

8 Lundby, C., Calbet, J. A., van Hall, G., Saltin, B. & Sander, M. Pulmonary gas exchange at maximal exercise in Danish lowlanders during 8 wk of acclimatization to 4,100 m and in high-altitude Aymara natives. *American journal of physiology. Regulatory, integrative and comparative physiology* **287**, R1202-1208, doi:10.1152/ajpregu.00725.2003 (2004).

9 Peng, Q. Q. *et al.* Physiological responses and evaluation of effects of BMI, smoking and drinking in high altitude acclimatization: a cohort study in Chinese Han young males. *PLoS One* **8**, e79346, doi:10.1371/journal.pone.0079346 (2013).

10 Parks, T., Brierley, G., Wilson, C. & Wolff, C. in *Proceedings of The Physiological Society.* (The Physiological Society).

11 Brown, J. P. R. & Grocott, M. P. W. Humans at altitude: physiology and pathophysiology. *Continuing Education in Anaesthesia, Critical Care & Pain* **13**, 17-22, doi:10.1093/bjaceaccp/mks047 (2013).

12 Clarke, A. *Harper's Practical Genetic Counselling.*, (CRC Press, 2016).

13 Inglese, P. *et al.* Deep learning and 3D-DESI imaging reveal the hidden metabolic heterogeneity of cancer. *Chem Sci* **8**, 3500-3511, doi:10.1039/c6sc03738k (2017).

14 Ried, J. S. *et al.* A principal component meta-analysis on multiple anthropometric traits identifies novel loci for body shape. *Nat Commun* **7**, 13357, doi:10.1038/ncomms13357 (2016).

15 Holmes, E. *et al.* Human metabolic phenotype diversity and its association with diet and blood pressure. *Nature* **453**, 396-400, doi:10.1038/nature06882 (2008).

16 Yang, J. *et al.* Conditional and joint multiple-SNP analysis of GWAS summary statistics identifies additional variants influencing complex traits. *Nat Genet* **44**, 369-375, S361-363, doi:10.1038/ng.2213 (2012).

17 Aschard, H. *et al.* Maximizing the power of principal-component analysis of correlated phenotypes in genome-wide association studies. *Am J Hum Genet* **94**, 662-676, doi:10.1016/j.ajhg.2014.03.016 (2014).

18 Li, F. *et al.* A powerful latent variable method for detecting and characterizing gene-based gene-gene interaction on multiple quantitative traits. *BMC Genet* **14**, 89, doi:10.1186/1471-2156-14-89 (2013).

19 Zhang, X. *et al.* A PLSPM-based test statistic for detecting gene-gene co-association in genome-wide association study with case-control design. *PLoS One* **8**, e62129, doi:10.1371/journal.pone.0062129 (2013).

20 Sanchez, G. PLS path modeling with R. *Berkeley: Trowchez Editions* (2013).

21 Tenenhaus, M., Vinzi, V. E., Chatelin, Y.-M. & Lauro, C. PLS path modeling. *Computational statistics & data analysis* **48**, 159-205 (2005).

22 by Endo, T.-B. D. M. Handbook of partial least squares.

23 Hastie, T., Tibshirani, R. & Friedman, J. (Springer, 2009).

24 Von Luxburg, U. A tutorial on spectral clustering. *Statistics and computing* **17**, 395-416 (2007).

25 Macqueen, J. B. in *Procedings of the Fifth Berkeley Symposium on Math, Statistics, and Probability.* 281-297 (University of California Press).

26 Freedman, D. *Statistical Models: Theory and Practice*. (Cambridge University Press, 2009).

27 Dawkins, R. Replicator selection and the extended phenotype. *Z Tierpsychol* **47**, 61-76 (1978).

28 Fitzmaurice, G. M., Laird, N. M. & Ware, J. H. *Applied longitudinal analysis*. Vol. 998 (John Wiley & Sons, 2012).

29 Zelnik-Manor, L. & Perona, P. Self-tuning spectral clustering. (2005).

30 Akaike, H. in *Selected Papers of Hirotugu Akaike* 199-213 (Springer, 1998).

31 Aho, K., Derryberry, D. & Peterson, T. Model selection for ecologists: the worldviews of AIC and BIC. *Ecology* **95**, 631-636 (2014).

32 Schwarz, G. Estimating the dimension of a model. *The annals of statistics* **6**, 461-464 (1978).

33 Kohavi, R. in *Ijcai.* 1137-1145 (Stanford, CA).

34 Hyndman, R. J. & Koehler, A. B. Another look at measures of forecast accuracy. *International Journal of Forecasting* **22**, 679-688, doi:10.1016/j.ijforecast.2006.03.001 (2006).

35 Team, R. C. R: A language and environment for statistical computing. (2013).

36 Works, M. Matlab User Manual Version r2015b. *Math Works Incorporation, Natick, MA* (2015).

37 Wickham, H. *ggplot2: elegant graphics for data analysis*. (Springer Science & Business Media, 2009).

38 Csardi, G. & Nepusz, T. The igraph software package for complex network research. *InterJournal, Complex Systems* **1695**, 1-9 (2006).

39 Kassambara, A. & Mundt, F. Factoextra: extract and visualize the results of multivariate data analyses. *R package version* **1** (2016).

40 Charrad, M., Ghazzali, N., Boiteau, V. & Niknafs, A. Nbclust: An R Package for Determining the Relevant Number of Clusters in a Data Set. *J Stat Softw* **61**, 1-36 (2014).

41 Goeman, J. J. & Solari, A. Multiple hypothesis testing in genomics. *Stat Med* **33**, 1946-1978, doi:10.1002/sim.6082 (2014).

42 Wilcoxon, F. Individual Comparisons by Ranking Methods. *Biometrics Bulletin* **1**, 80, doi:10.2307/3001968 (1945).

43 Myers, J. L., Well, A. & Lorch, R. F. *Research design and statistical analysis*. (Routledge, 2010).

44 Altman, N. S. An Introduction to Kernel and Nearest-Neighbor Nonparametric Regression. *The American Statistician* **46**, 175, doi:10.2307/2685209 (1992).

45 Rousseeuw, P. J. Silhouettes: A graphical aid to the interpretation and validation of cluster analysis. *J Comput Appl Math* **20**, 53-65, doi:10.1016/0377-0427(87)90125-7 (1987).

46 Pearson, K. Note on regression and inheritance in the case of two parents. *Proceedings of the Royal Society of London* **58**, 240-242 (1895).

47 Roach, R., Bartsch, P., Hackett, P. & Oelz, O. The Lake Louise acute mountain sickness scoring system. *Hypoxia and molecular medicine* **272**, 4 (1993).

48 Calbet, J. A. L. *et al.* Effect of blood haemoglobin concentration on V̇o2,maxand cardiovascular function in lowlanders acclimatised to 5260 m. *The Journal of Physiology* **545**, 715-728, doi:10.1113/jphysiol.2002.029108 (2002).

49 Vij, A. G. Effect of prolonged stay at high altitude on platelet aggregation and fibrinogen levels. *Platelets* **20**, 421-427, doi:10.1080/09537100903116516 (2009).

50 Hackett, P. H., Schoene, R. B., Winslow, R. M., Peters, R. M., Jr. & West, J. B. Acetazolamide and exercise in sojourners to 6,300 meters--a preliminary study. *Med Sci Sports Exerc* **17**, 593-597 (1985).

51 Winslow, R. M. R. M. & Monge, C. *Hypoxia, polycythemia and chronic mountain sickness*. (1987).

52 Fisher, R. A. On the probable error of a coefficient of correlation deduced from a small

sample. *Metron* **1**, 3-32 (1921).

53 Fisher, R. A. in *Breakthroughs in Statistics* 66-70 (Springer, 1992).

54 Cohen, J., Cohen, P., West, S. G. & Aiken, L. S. *Applied multiple regression/correlation analysis for the behavioral sciences*. (Routledge, 2013).

55 Diedenhofen, B. & Musch, J. cocor: a comprehensive solution for the statistical comparison of correlations. *PLoS One* **10**, e0121945, doi:10.1371/journal.pone.0121945 (2015).

56 Burtscher, M., Szubski, C. & Faulhaber, M. Prediction of the susceptibility to AMS in simulated altitude. *Sleep Breath* **12**, 103-108, doi:10.1007/s11325-007-0131-0 (2008).

57 Karinen, H. M., Peltonen, J. E., Kahonen, M. & Tikkanen, H. O. Prediction of acute mountain sickness by monitoring arterial oxygen saturation during ascent. *High Alt Med Biol* **11**, 325-332, doi:10.1089/ham.2009.1060 (2010).

58 Koehle, M. S., Guenette, J. A. & Warburton, D. E. Oximetry, heart rate variability, and the diagnosis of mild-to-moderate acute mountain sickness. *Eur J Emerg Med* **17**, 119-122, doi:10.1097/MEJ.0b013e32832fa099 (2010).

59 Brierley, G., Parks, T. & Wolff, C. in *Oxygen Transport to Tissue XXXIII* 207-212 (Springer, 2012).

60 Verbeke, G. & Molenberghs, G. *Linear mixed models for longitudinal data*. (Springer Science & Business Media, 2009).

61 Richalet, J. P., Larmignat, P., Poitrine, E., Letournel, M. & Canoui-Poitrine, F. Physiological risk factors for severe high-altitude illness: a prospective cohort study. *Am J Respir Crit Care Med* **185**, 192-198, doi:10.1164/rccm.201108-1396OC (2012).

62 Wei, W. H., Hemani, G. & Haley, C. S. Detecting epistasis in human complex traits. *Nat Rev Genet* **15**, 722-733, doi:10.1038/nrg3747 (2014).

63 Houle, D., Govindaraju, D. R. & Omholt, S. Phenomics: the next challenge. *Nat Rev Genet* **11**, 855-866, doi:10.1038/nrg2897 (2010).

64 Zbuk, K. M. & Eng, C. Cancer phenomics: RET and PTEN as illustrative models. *Nat Rev Cancer* **7**, 35-45, doi:10.1038/nrc2037 (2007).

FIGURE LEGENDS:

Figure 1. The workflow and design of this study.

Figure 2. The absolute value of spearman correlation heatmap of 28 physiological phenotypes. The spearman correlation coefficient ranges from 0 (dark blue) to 1 (dark red). The spectral clustering results are marked by white boxes. For example, SBP and DBP are grouped together, and their absolute spearman correlation coefficient is about 0.6 (yellow-green color).

Figure 3. The PLSPM loadings of 14 composite phenotypes of high altitude acclimatization. The 14 composite phenotypes (LV1, …, LV14) are represented by 14 different colors, and the height of each colorful bar is the loading (correlation) of each composite phenotype. Acceptable values for the loadings are values greater than 0.7 (threshold line), indicating that more than 49% (0.7 x 0.7) of the variability in a single phenotype (like SBP or DBP) is captured by its composite phenotype (like LV3).

Figure 4. K-means clustering results on individuals using the 14 composite phenotypes (LVs). The 883 individuals are clustered as two groups (group 1 with 508 individuals and group 2 with 375 individuals) based on their composite phenotype scores. The PCA plot is just visualization of the k-means clustering results (group 1 with red color and group 2 with blue color accordingly).

Figure 5. The pairwise Pearson correlation heatmap of 14 composite phenotypes (LV1,…, LV14) of two groups. The Pearson correlation coefficient ranges from -1 (blue) to 1(red). The left figure represents the Pearson correlation heatmap of 14 LVs of group 1 and the right figure represents the Pearson correlation heatmap of 14 LVs of group 2.

Supplementary Figure 1. The eigenvalue gap of spectral clustering. The eigenvalue gap was maximized to choose the best number of spectral clustering (red line). And the best clustering number is 14.

Supplementary Figure 2. The 14 composite phenotypes of high altitude acclimatization. The numbers on the arrows are the PLSPM loadings of 14 composite phenotypes, which is the same as Figure 3.

Supplementary Figure 3. The optimal number of k-means clustering on individuals. The optimal number of clusters is 2 following the majority rule of total 26 clustering indices.

Supplementary Figure 4. The silhouette plot of k-means clustering on individuals. Silhouette values range from 1 to -1, when silhouette value is close to 1 indicating that the individuals are well clustered. The silhouette plot for k-means clustering showed that observations are well clustered.

Supplementary Figure 5. The histogram plot and density plot of each LV (14 LVs) between 2 groups (group 1 with red color and group 2 with blue color). And we further calculated the Wilcoxon Rank Sum test pvalue (the title of histogram plot) of each LV between 2 groups.

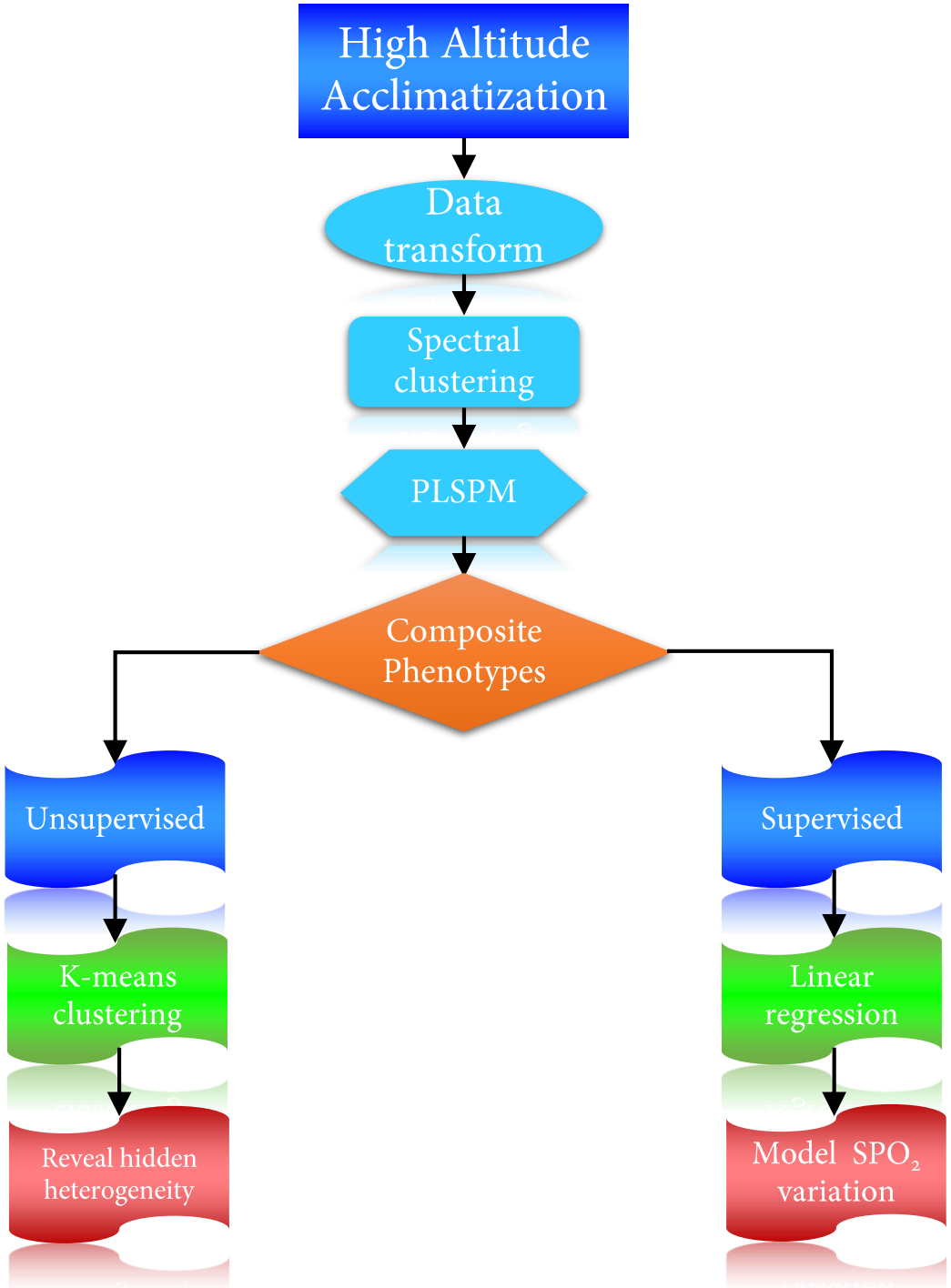
High Altitude Acclimatization
Data transform
Spectral clustering
PLSPM
Composite Phenotypes
Unsupervised
Supervised
K-means clustering
Linear regression
Reveal hidden heterogeneity
Model SPO_2 variation

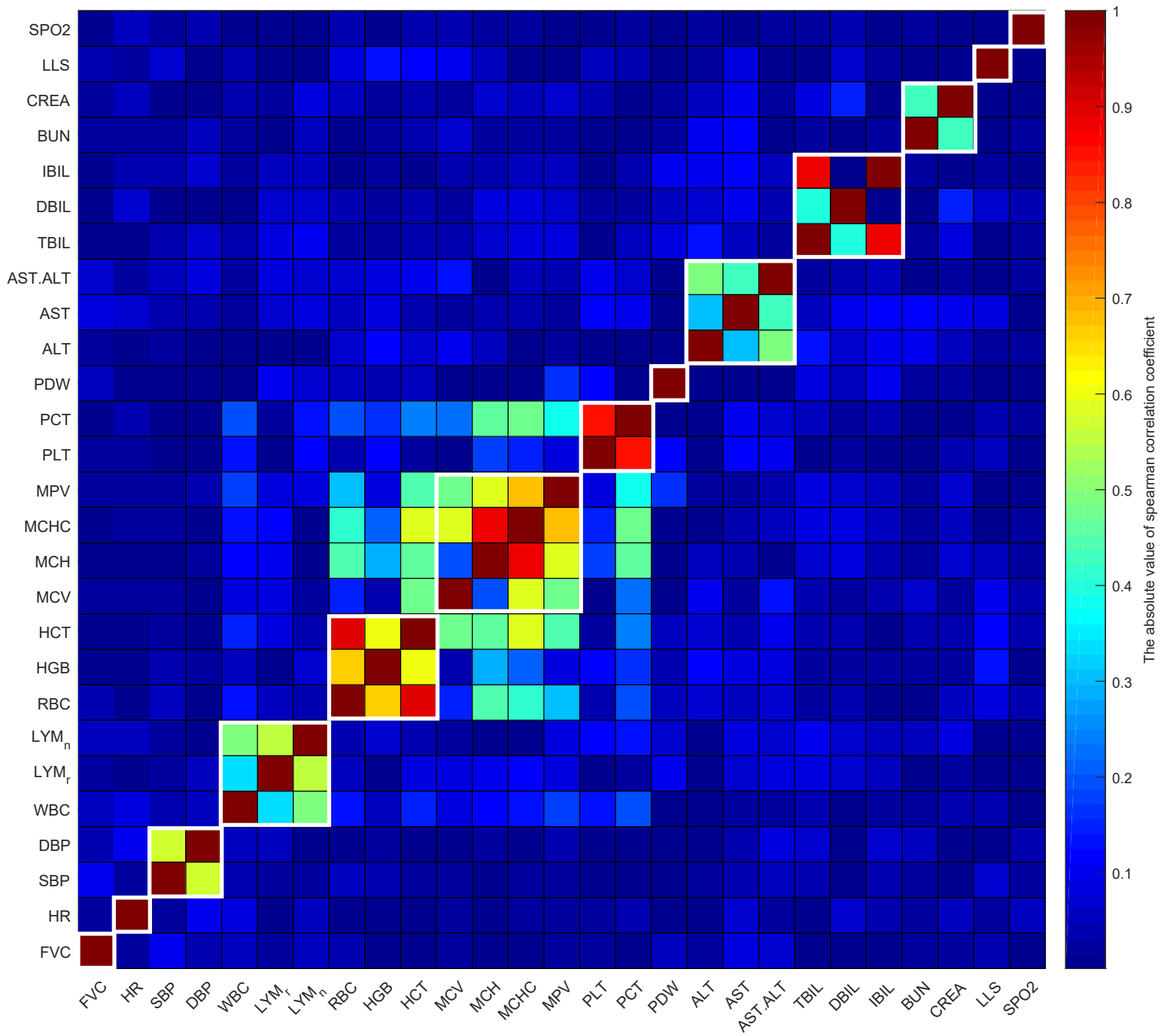
SPO2
LLS
CREA
BUN
IBIL
DBIL
TBIL
AST.ALT
AST
ALT
PDW
PCT
PLT
MPV
MCHC
MCH
MCV
HCT
HGB
RBC
LYM$_n$
LYM$_r$
WBC
DBP
SBP
HR
FVC
FVC HR SBP DBP WBC LYM$_r$ LYM$_n$ RBC HGB HCT MCV MCH MCHC MPV PLT PCT PDW ALT AST AST.ALT TBIL DBIL IBIL BUN CREA LLS SPO2
1
0.9
0.8
0.7
0.6
0.5
0.4
0.3
0.2
0.1
The absolute value of spearman correlation coefficient

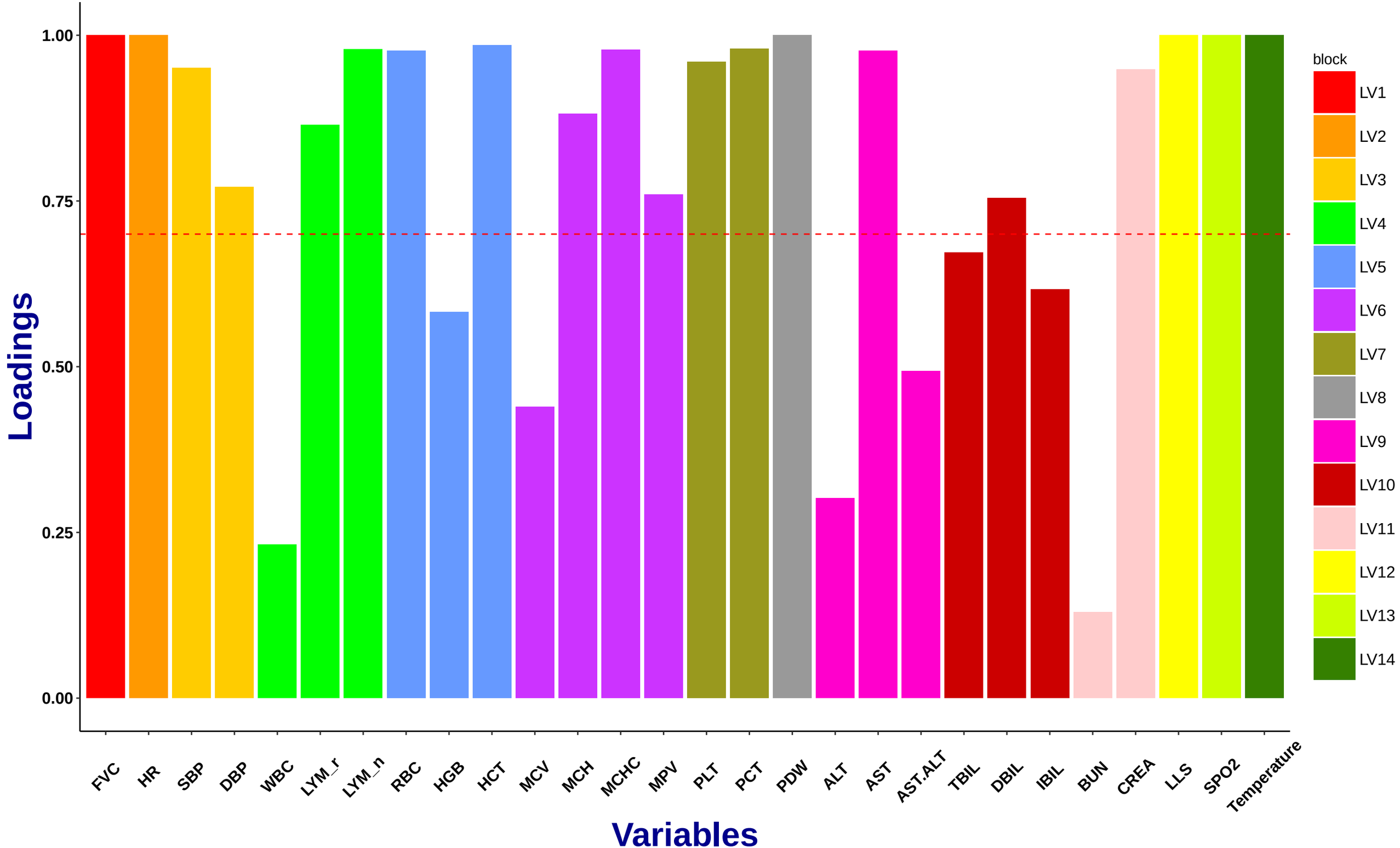
Loadings
1.00
0.75
0.50
0.25
0.00
FVC
HR
SBP
DBP
WBC
LYM_r
LYM_n
RBC
HGB
HCT
MCV
MCH
MCHC
MPV
PLT
PCT
PDW
ALT
AST
AST.ALT
TBIL
DBIL
IBIL
BUN
CREA
LLS
SPO2
Temperature
Variables
block
LV1
LV2
LV3
LV4
LV5
LV6
LV7
LV8
LV9
LV10
LV11
LV12
LV13
LV14

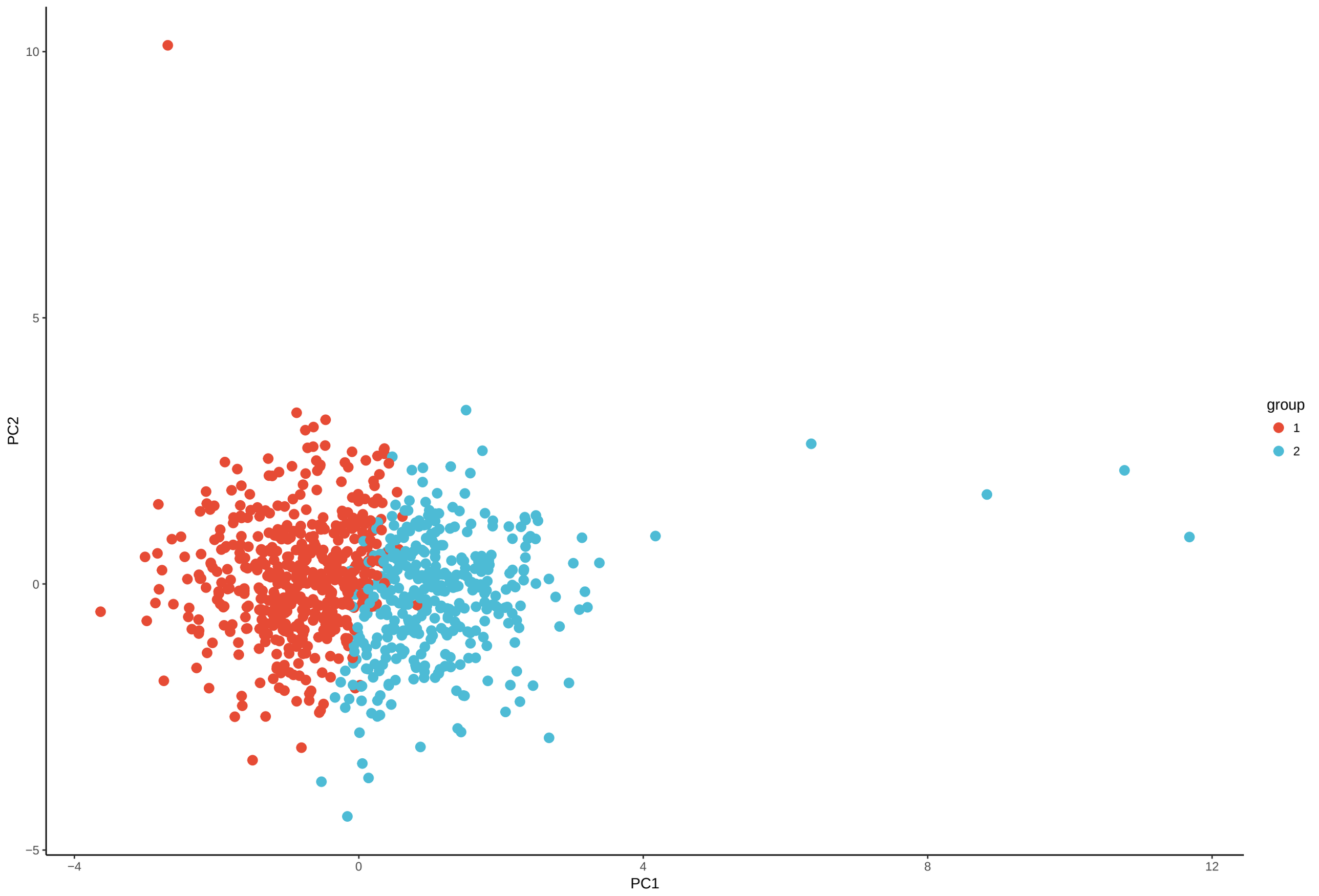
10
5
0
−5
PC2
−4
0
4
8
12
PC1
group
1
2

Group 1

	LV1	LV2	LV3	LV4	LV5	LV6	LV7	LV8	LV9	LV10	LV11	LV12	LV13	LV14
LV14														1
LV13													1	−0.03
LV12												1	−0.07	0.01
LV11											1	−0.04	0.05	−0.09
LV10										1	0.1	−0.01	−0.06	0.09
LV9									1	−0.09	−0.07	−0.02	−0.01	−0.04
LV8								1	0	−0.03	−0.06	0.06	−0.03	−0.02
LV7							1	−0.06	−0.04	0.07	0.13	0.04	−0.02	0.14
LV6						1	0.12	0.22	−0.19	0.06	0.08	−0.01	0.12	0.14
LV5					1	0.18	−0.2	0.09	−0.06	0.1	0.12	0.02	0.03	−0.05
LV4				1	−0.06	−0.02	0.07	−0.09	0.08	0.06	0.02	−0.08	−0.02	−0.01
LV3			1	−0.02	−0.05	0.01	−0.03	0.01	0	−0.02	−0.02	0.09	−0.07	0.09
LV2		1	0.07	0.06	0.08	0.1	0.03	−0.02	−0.13	0.12	0.05	0.04	−0.08	0.04
LV1	1	0.01	−0.05	−0.02	0.01	0.05	−0.05	0.04	−0.04	0.01	−0.01	−0.04	0.01	−0.01

Pearson Correlation: 1.0, 0.5, 0.0, −0.5, −1.0

Group 2

	LV1	LV2	LV3	LV4	LV5	LV6	LV7	LV8	LV9	LV10	LV11	LV12	LV13	LV14
LV14														1
LV13													1	0.04
LV12												1	−0.1	−0.02
LV11											1	0.04	−0.07	0.08
LV10										1	0.07	0.04	−0.06	0
LV9									1	−0.07	−0.18	0.08	0.07	−0.06
LV8								1	0	0.03	0.02	−0.05	−0.04	0.05
LV7							1	0.01	0.06	0.03	0.11	0.06	0.02	0.07
LV6						1	0.21	0.07	−0.35	0.05	0.18	0.02	−0.03	0.18
LV5					1	0.52	0.17	0.18	−0.18	0.02	0.07	0.04	0.02	0
LV4				1	−0.05	−0.04	0.09	−0.11	0.09	0.03	0.05	0.05	−0.03	−0.01
LV3			1	0.08	−0.01	−0.05	0.01	−0.02	−0.08	0.04	0.05	−0.03	0.09	0.11
LV2		1	0.06	0.01	0.06	0.07	0.15	0.01	0.07	0.03	0.03	0.06	−0.04	−0.07
LV1	1	0	−0.05	−0.03	0.01	−0.04	0.05	0.05	0.01	0.07	0.01	0.04	−0.07	−0.04

Pearson Correlation: 1.0, 0.5, 0.0, −0.5, −1.0

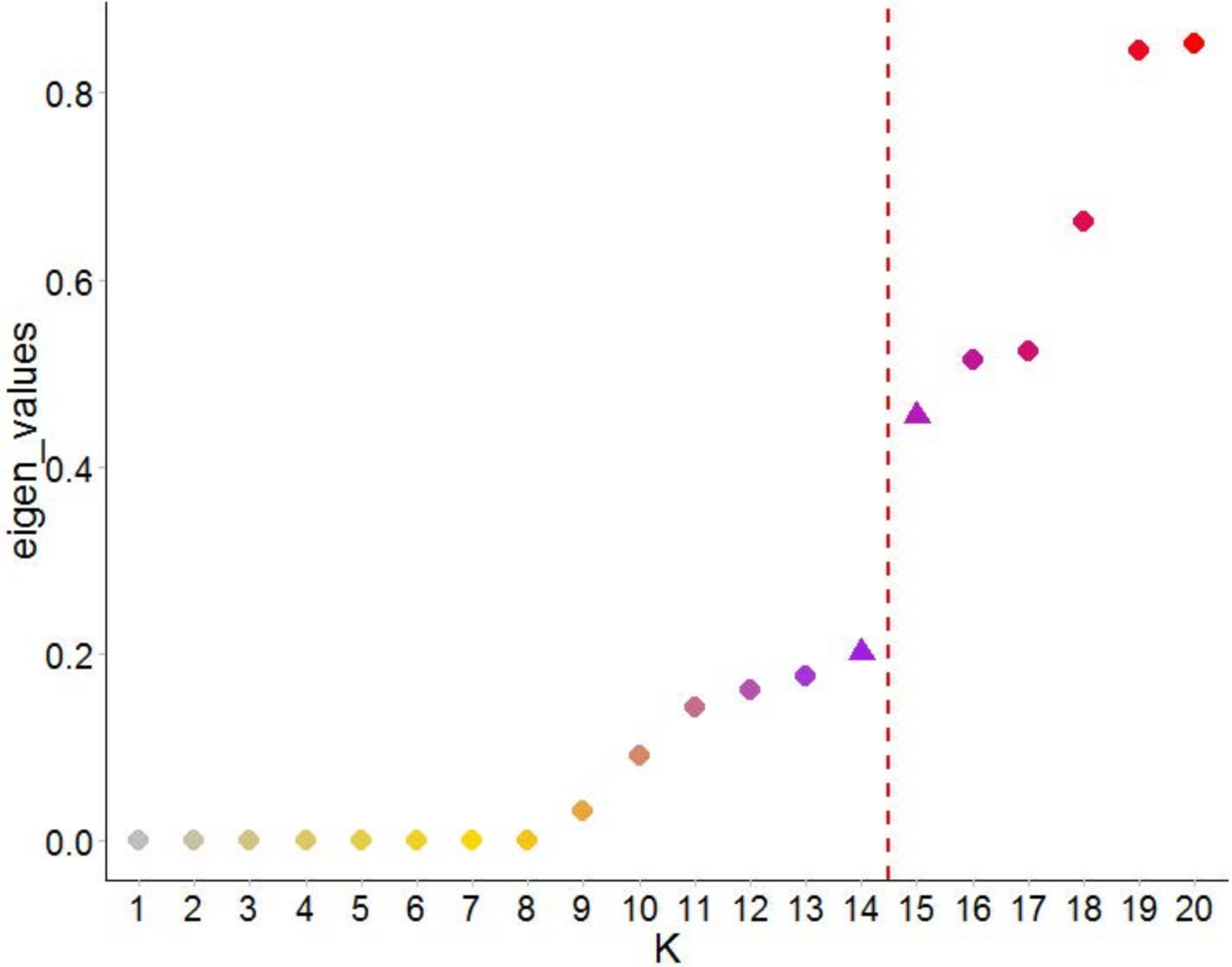
eigen_values
0.0
0.2
0.4
0.6
0.8
1
2
3
4
5
6
7
8
9
10
11
12
13
14
15
16
17
18
19
20
K

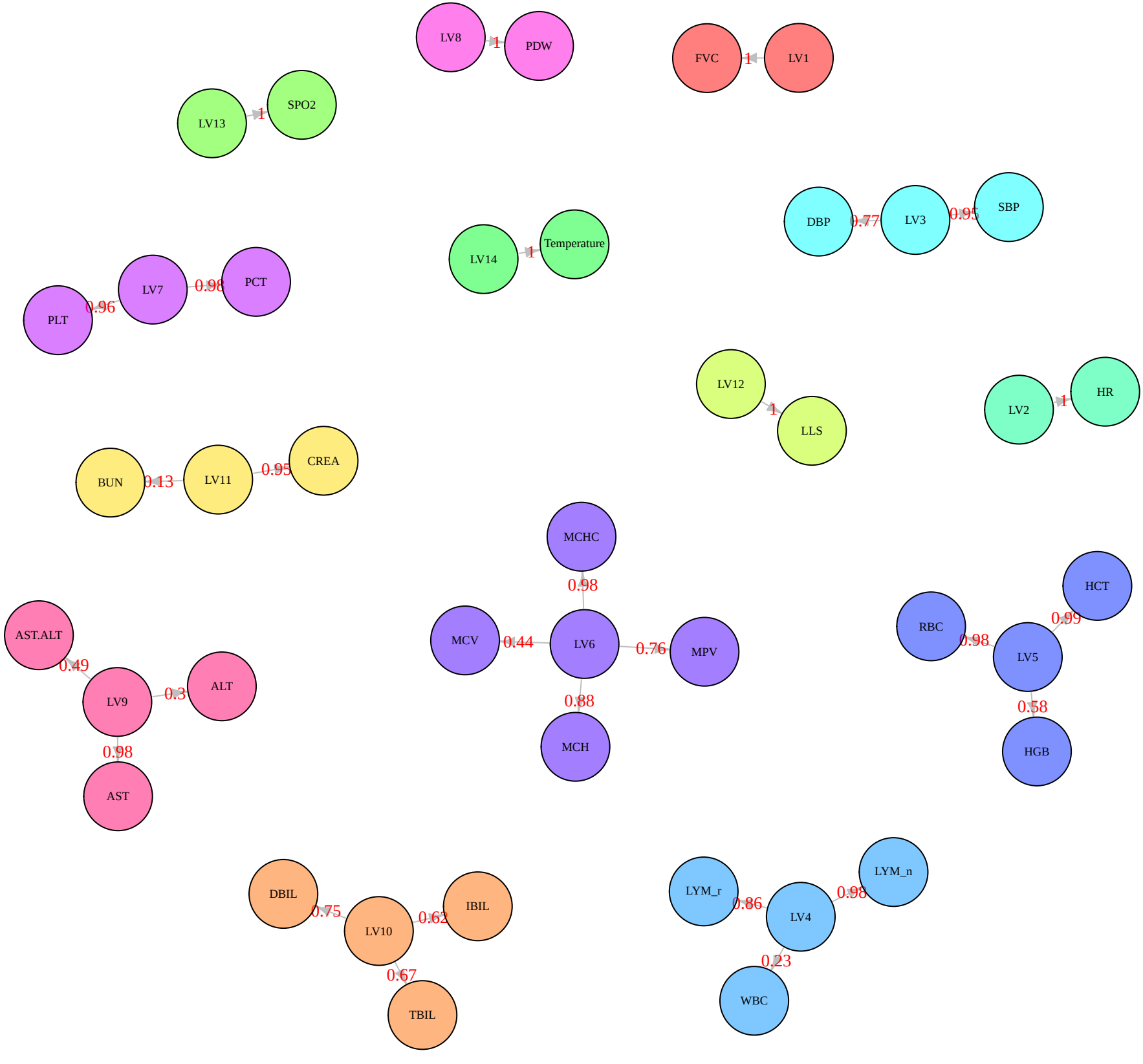
LV8
1
PDW
FVC
1
LV1
LV13
1
SPO2
DBP
0.77
LV3
0.95
SBP
LV14
1
Temperature
PLT
0.96
LV7
0.98
PCT
LV12
1
LLS
LV2
1
HR
BUN
0.13
LV11
0.95
CREA
MCHC
0.98
MCV
0.44
LV6
0.76
MPV
0.88
MCH
HCT
0.99
RBC
0.98
LV5
0.58
HGB
AST.ALT
0.49
LV9
0.3
ALT
0.98
AST
DBIL
0.75
LV10
0.62
IBIL
0.67
TBIL
LYM_r
0.86
LV4
0.98
LYM_n
0.23
WBC

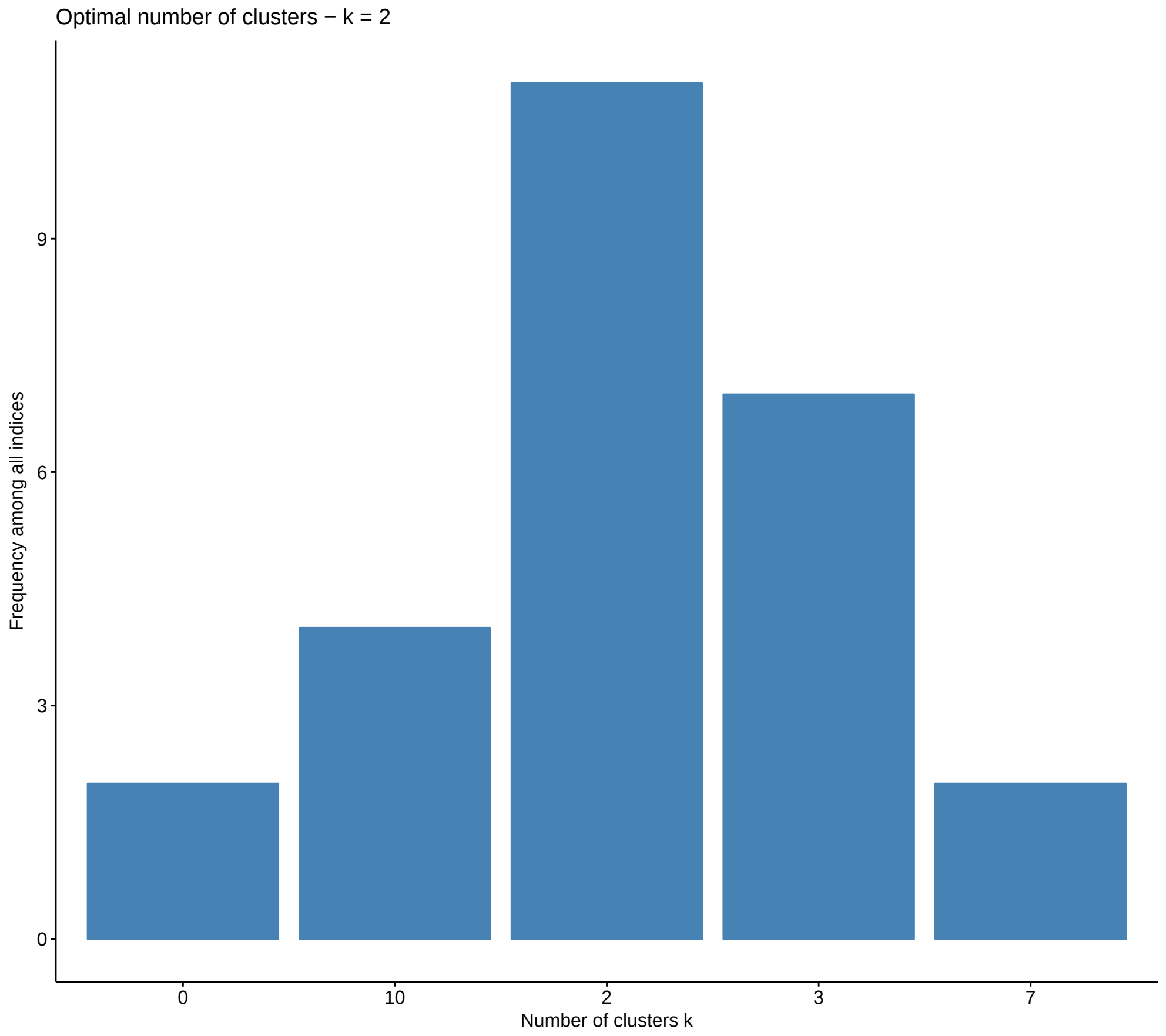
Optimal number of clusters − k = 2
Frequency among all indices
0
3
6
9
0
10
2
3
7
Number of clusters k

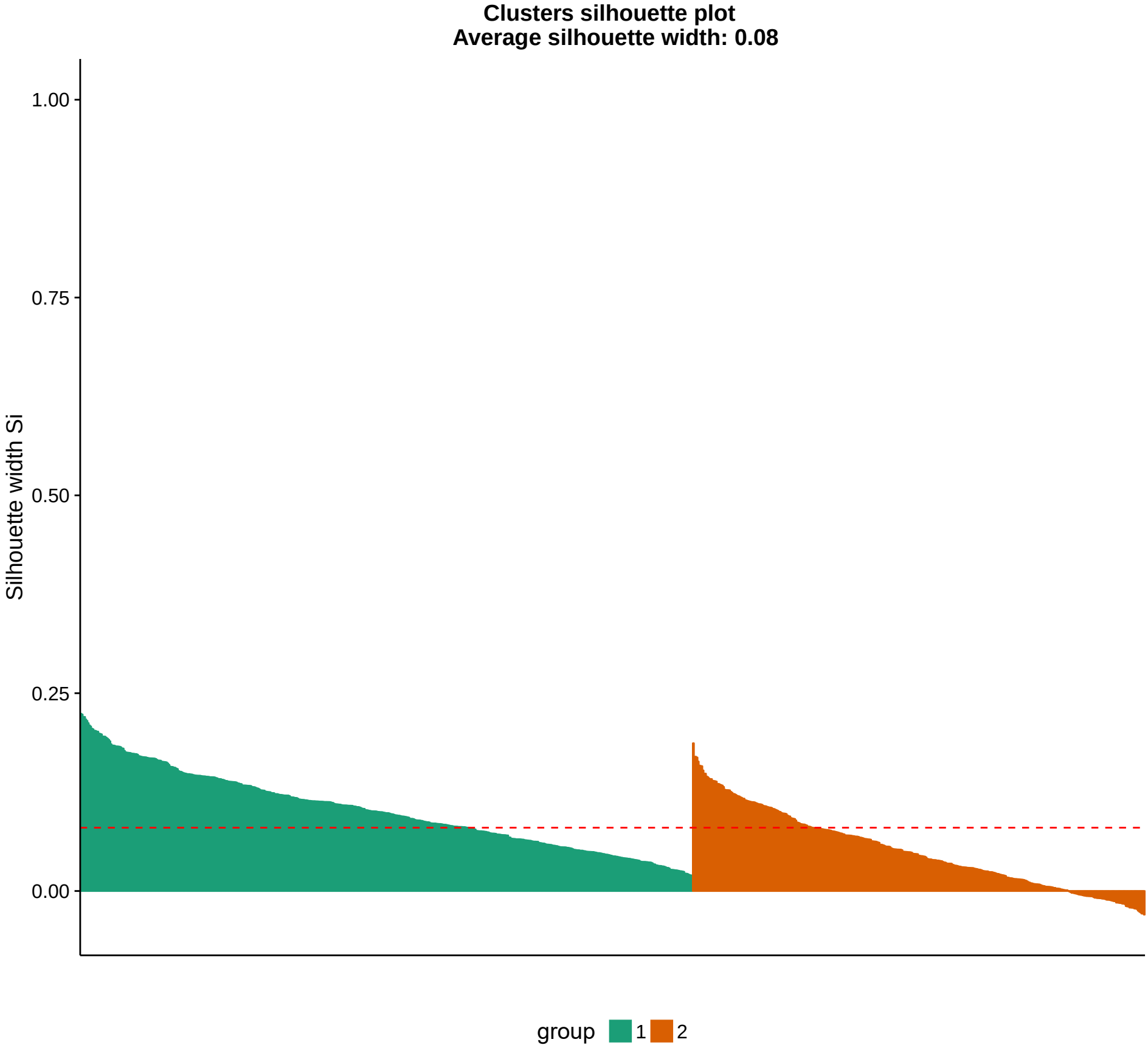
Clusters silhouette plot
Average silhouette width: 0.08
Silhouette width Si
1.00
0.75
0.50
0.25
0.00
group
1
2

The Wilcoxon Rank Sum Test's pvalue is 0.7481004544445422

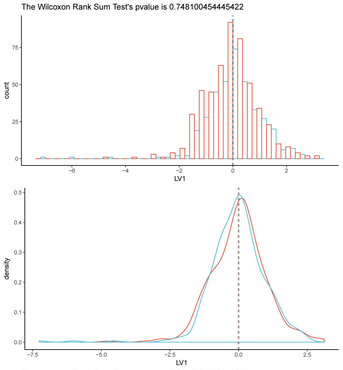

The Wilcoxon Rank Sum Test's pvalue is 0.0348616218786328

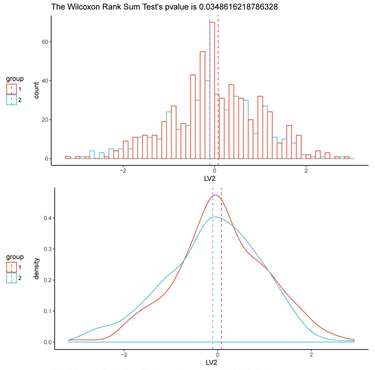

The Wilcoxon Rank Sum Test's pvalue is 0.539766496579975

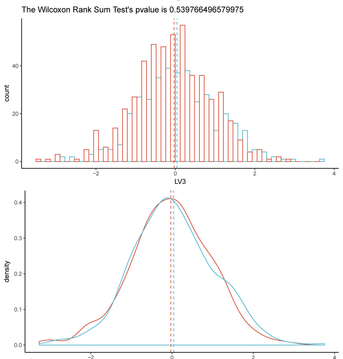

The Wilcoxon Rank Sum Test's pvalue is 0.850933712542198

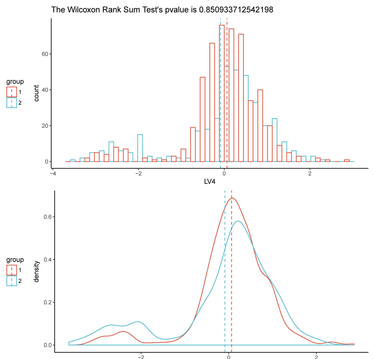

The Wilcoxon Rank Sum Test's pvalue is 3.67803192810894e−75

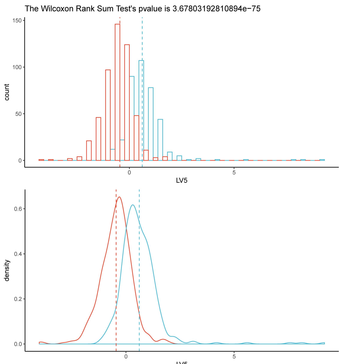

The Wilcoxon Rank Sum Test's pvalue is 3.35761232058996e−90

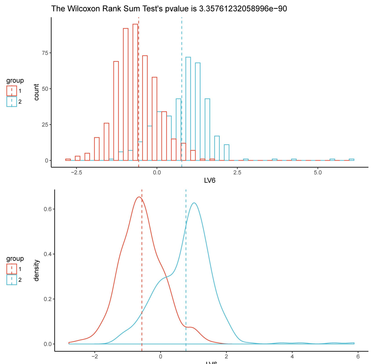

The Wilcoxon Rank Sum Test's pvalue is 2.31110505988706e−37

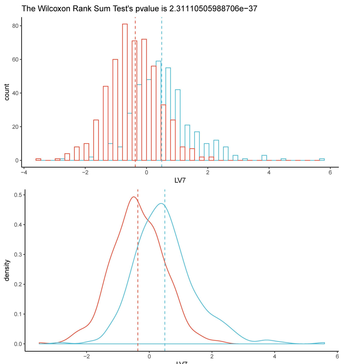

The Wilcoxon Rank Sum Test's pvalue is 0.234379416894722

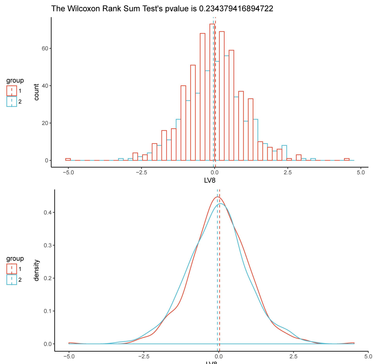

The Wilcoxon Rank Sum Test's pvalue is 4.2205517907523e−10

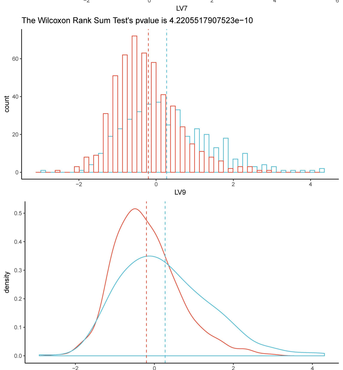

The Wilcoxon Rank Sum Test's pvalue is 5.51437750854521e−08

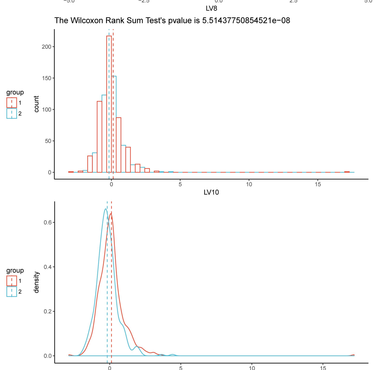

The Wilcoxon Rank Sum Test's pvalue is 9.22248315597901e−10

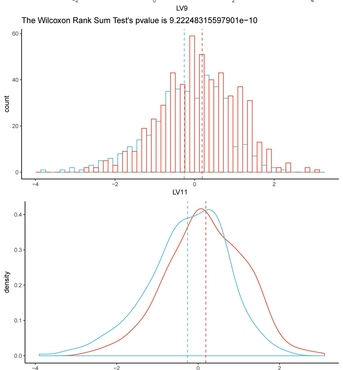

The Wilcoxon Rank Sum Test's pvalue is 0.0347443927692118

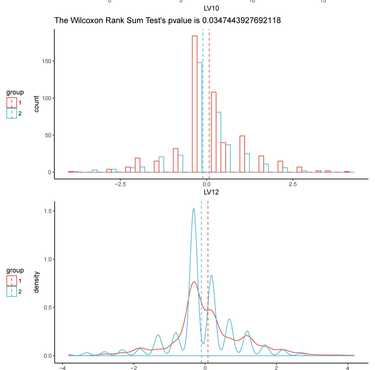

The Wilcoxon Rank Sum Test's pvalue is 0.027167025618282

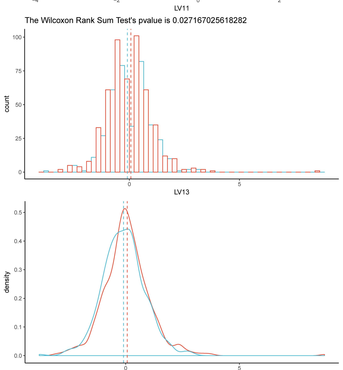

The Wilcoxon Rank Sum Test's pvalue is 6.17426754739736e−05

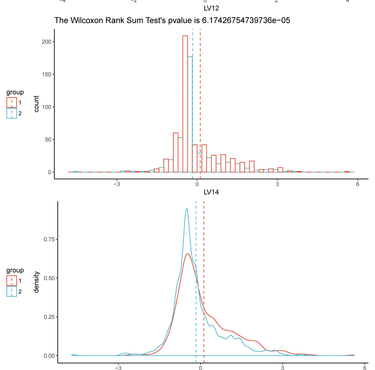

Table 1. The 28 physiological traits from 883 Chinese Han young males at baseline and chronic phases of high altitude acclimatization.

Variables	Baseline		Chronic		Pvalue*
	Mean	Sd	Mean	Sd	
ALT	19.11	8.14	15.02	9.08	**6.28E-45**
AST	15.64	5.83	46.05	15.24	**2.33E-139**
AST.ALT	0.85	0.18	3.91	2.54	**2.14E-139**
TBIL	11.94	1.77	14.51	24.90	**1.41E-10**
DBIL	2.69	0.61	5.70	1.70	**3.72E-136**
IBIL	9.25	1.24	8.81	24.95	**1.96E-39**
BUN	5.08	1.12	6.21	1.17	**3.20E-87**
CREA	58.32	10.38	113.02	12.20	**2.85E-139**
WBC	6.21	1.34	8.21	1.70	**1.55E-125**
LYM%	36.16	7.48	40.61	10.71	**7.71E-42**
LYM#	2.21	0.52	3.31	0.99	**1.78E-106**
RBC	4.88	0.39	5.73	0.48	**5.25E-144**
HGB	150.15	10.05	179.59	13.46	**2.07E-144**
HCT	0.44	0.03	0.50	0.04	**1.35E-136**
MCV	90.60	5.14	87.39	4.89	**6.49E-126**
MCH	30.91	2.34	31.39	2.18	**1.16E-21**
MCHC	341.07	17.94	359.14	16.24	**3.97E-85**
PLT	206.88	42.79	258.94	51.49	**2.18E-124**
PCT	2.01	0.42	2.72	0.51	**9.95E-139**
MPV	9.78	1.26	10.54	0.62	**9.59E-68**
PDW	13.79	2.25	18.03	2.53	**9.71E-142**
FVC	444.45	38.26	412.31	59.16	**2.03E-51**
SBP	110.88	10.45	124.34	12.94	**2.51E-87**
DBP	73.21	8.65	75.98	9.61	**7.46E-13**
HR	66.49	9.57	87.16	10.99	**3.24E-123**
Temperature	36.22	0.12	36.38	0.29	**1.75E-39**
SPO2	97.76	2.08	85.82	3.80	**6.64E-132**
LLS	0.88	1.59	1.40	1.73	**1.14E-10**

*** Pvalues were calculated by Wilcoxon Rank-Sum Test (paired= true).**

The significant (under Bonferroni correction) pvalues were shown in bold.

Table 2. PLSPM composite phenotypes unidimensionality evaluation.

	Biological Meanings	Manifest variables	Mode	MVs	C.alpha	DG.rho	eig.1st	eig.2nd
LV1	forced vital capacity	FVC	A	1	1.00	1.00	1.00	0.00
LV2	heart rate	HR	A	1	1.00	1.00	1.00	0.00
LV3	blood pressure	SBP, DBP	A	2	0.70	0.87	1.54	0.46
LV4	immune system	LYM#, LYM%, WBC	A	3	0.55	0.77	1.76	1.21
LV5	number of red cells	RBC, HCT, HGB	A	3	0.89	0.93	2.45	0.48
LV6	hemoglobin concentration	MCH, MCHC, MPV, MCV	A	4	0.79	0.87	2.52	1.01
LV7	number of platelets	PLT, PCT	A	2	0.94	0.97	1.88	0.12
LV8	platelet distribution width	PDW	A	1	1.00	1.00	1.00	0.00
LV9	liver function	ALT, AST, AST/ALT	A	3	0.25	0.04	1.35	1.31
LV10	bilirubin	TBIL, DBIL, IBIL	A	3	0.59	0.79	2.00	1.00
LV11	renal function	BUN, CREA	A	2	0.61	0.84	1.44	0.56
LV12	Lake Louise score	LLS	A	1	1.00	1.00	1.00	0.00
LV13	oxygen saturation	SPO_2	A	1	1.00	1.00	1.00	0.00
LV14	body temperature	body temperature	A	1	1.00	1.00	1.00	0.00

Note: Overall 14 composite phenotypes are shown as the latent variables (**LV1, LV2**…**LV13, LV14**).

Table 3. Evaluation the goodness of fit of two multivariate linear regression models.

	Model1 (original variables)	Model2 (LV)	Pvalue*
AIC	5089	**5069**	_
BIC	5227	**5141**	_
10 fold CV RMSE	4.32	**4.26**	_
10 fold CV MSE (SD)	18.64 (5.60)	**18.12 (5.71)**	**0.00488**
Leave one out CV RMSE	4.32	**4.265**	_
Leave one out CV MSE (SD)	18.66 (53.42)	**18.19 (53.32)**	**0.00294**

*The Pvalues were calculated by Wilcoxon Rank-Sum Test.

The measurement indices with better fitness were shown in bold.

The significant pvalues (pvalue<0.05) were marked as bold and red color.